NJC

Accepted Manuscript

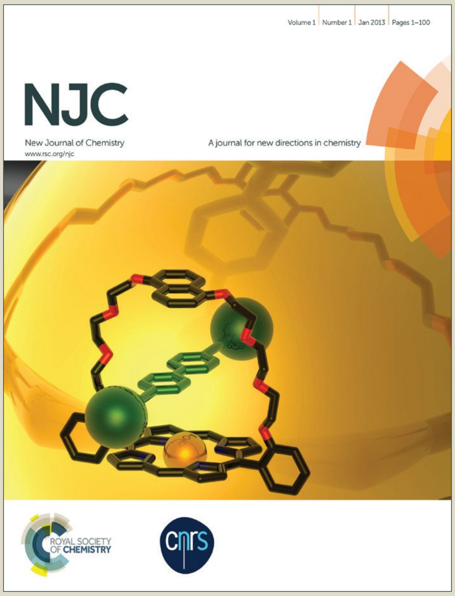

ROYAL SOCIETY OF CHEMISTRY

www.rsc.org/njc

Graphical abstract

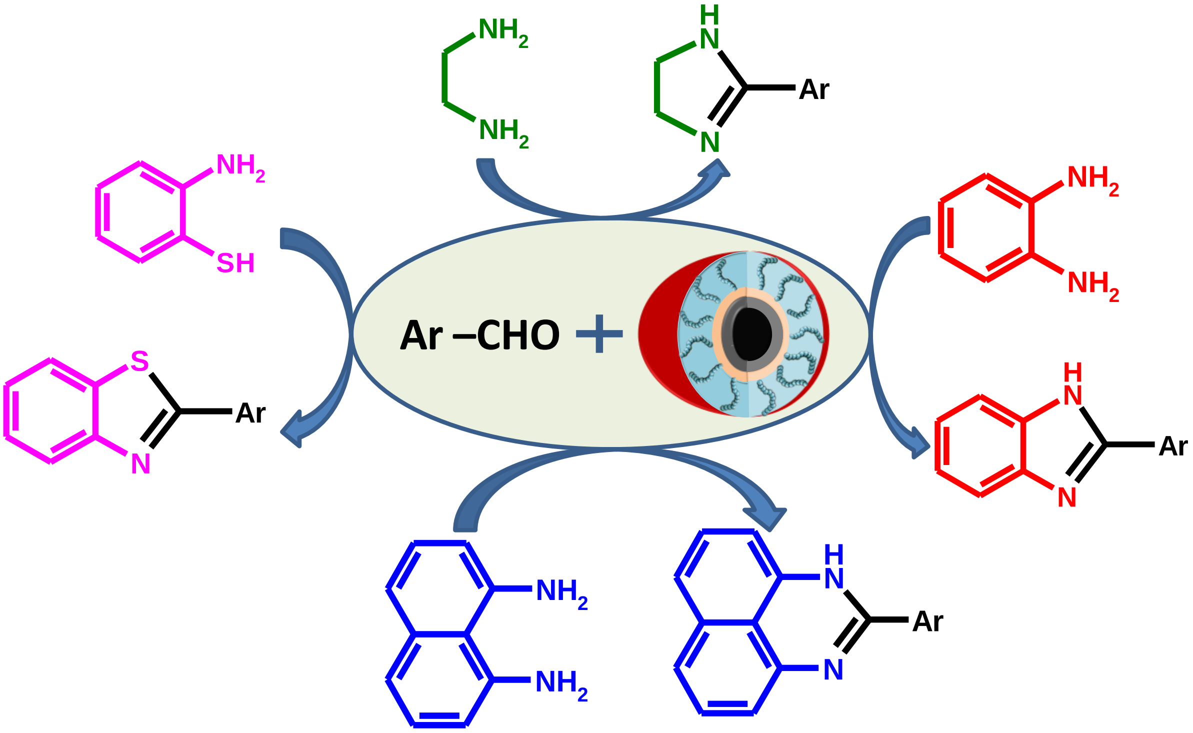

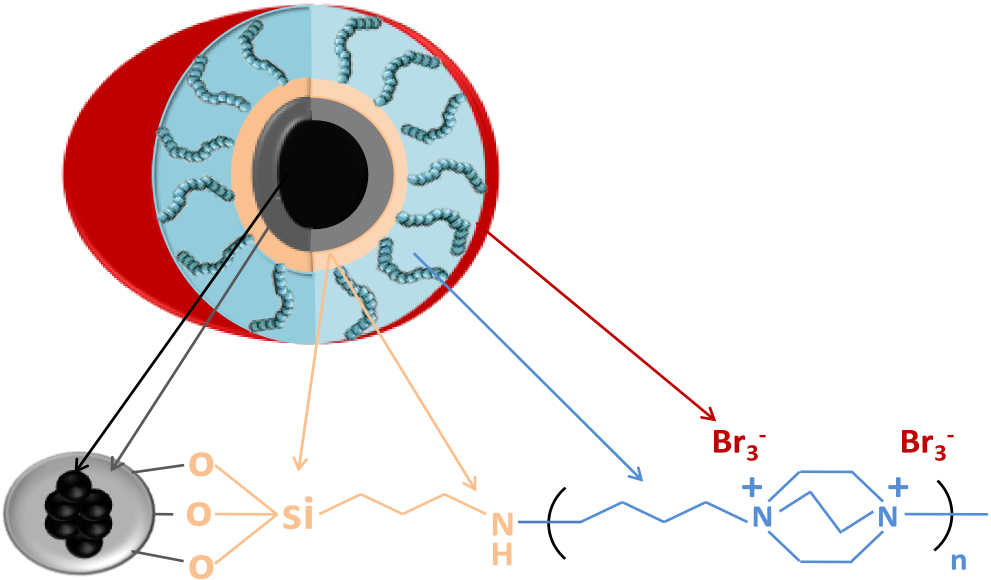

Fe_3O_4@SiO_2@PolyIonene/Br_3^- core–shell-shell magnetic nanoparticles : a novel catalyst for the synthesis of imidazole derivatives in solvent-free conditions

Elham Dezfoolinezhad[1,2], **Keivan Ghodrati**[3*], **Rashid Badri**[1,2]

[1] Department of Chemistry, Khuzestan Science and Research Branch, Islamic Azad University, Ahvaz, Iran

[2] Department of Chemistry, Ahvaz Branch, Islamic Azad University, Ahvaz, Iran

[3] Department of Chemistry, Kermanshah Branch, Islamic Azad University, Kermanshah. Iran

Abstract

A new Fe_3O_4@SiO_2@Polyionene/Br_3^- core–shell-shell magnetite nanoparticle was prepared with co-precipitation method and was used in the syntheses of imidazole derivatives in solvent-free conditions. The ionene was easily prepared with reacting DABCO and 1,4-dibromo butane in DMF/Methanol. The polyionene was added to the previous layers and magnetic core–shell nanoparticles (P-MNPs) were functionalized. All resulting nanoparticles were characterized by transmission electron microscopy (TEM), scanning electron microscopy (SEM), infrared spectroscopy (FTIR), X-ray diffraction (XRD), thermo gravimetric analysis (TGA), differential scanning calorimeter (DSC), and vibrating sample magnetometer (VSM). The catalyst was readily recovered by simple magnetic decantation and can be recycled several times with no significant loss of catalytic activity.

Key Words :Fe_3O_4@SiO_2@Polyionene/Br_3^-, Magnetic core, Magnetic separation, Ionene, solvent-free.

1- Introduction

In the past decade, magnetic micro and nanoparticles have attracted much attention because of their unique magnetic properties and widespread application in different fields. Magnetic nanoparticles are efficient, and readily available, and have high surface-area resulting in high catalyst loading capacity and outstanding stability to heterogeneous supports for catalysts preparation [1]. Most of supported nano catalysts are separated by filtration or centrifugation, which cause the loss of catalysts in many reactions. To overcome this drawback, magnetic nanoparticles have emerged as effective new supports for immobilization, because magnetic nanoparticle-supported catalysts can be separated from the reaction medium by an external permanent magnet [2]. Accordingly, the application of magnetic nano particles catalysis has become an interesting filed of research besides other advantages of nano catalysts. A series of functionalized magnetic nanoparticles (MNPs) have been employed in a range of organic transformations, showing excellent catalytic activities in oxidation [3], hydrogenation [4-7], C–C coupling [8-11], dihydroxylation of olefins [12], amination [13], nitrile hydration [14], and catalytic reaction [15] reactions .

Ionenes are polymers with alkyl ammonium centers and are strongly charged cationic polyelectrolytes whose ammonium groups are located on the polymer main chain. The ionene term was first introduced by Rembaum et al. [16]. They are produced by polycondensation reaction between two monomers a dihaloalkane and a diamine. These kinds of polymers extensively used as humidity sensors, fungicides, electric conductors, bactericides, anticoagulants, flocculants, catalysts, supported polymers, and stationary phase supports in chromatography [16-23]. In solution, ionenes exhibit behavior like polyelectrolytes with extended conformation. Most experiments using the ionenes have been carried out in solution and just a few tests have been carried out in solid state or solvent free condition.

Because of their biological activities [24] imidazols, thiazols, and perimidines and their derivatives are widely interesting. These compounds were usually produced by the reaction of carbonyl group with diamine, or aminothiol compounds, in the presence of a reagent [25]. However, most of these processes suffer some drawbacks such as strong acidic conditions, high cost, low yields of the products, long reaction time, and tedious work-up procedures, the use of toxic reagents, catalysts and/or solvents, reusability of the reagents, and instability in storage. Therefore, the development of a cost effective, and expansion of safe and environment friendly reagent system is desirable.

In connection with our ongoing work on application of magnetic nano particle, herein, we report the synthesis and characterization of recoverable and nano magnetically core-shell ionene layered tribromide and their catalytic application in the synthesis of some five- and six-member heterocycles. The fabrication procedure mainly involves six steps as shown in Scheme 1. The preparation first consists of magnetite particles synthesis by co-precipitation reaction of ferrous and ferric salts with NH_4OH. To avoid possible aggregation or oxidation of the iron oxide nanoparticles, a layer of SiO_2 was coated on the nanoparticles as the iron oxide surface has a strong affinity to silica. The surface modification of these particles was performed through the grafting of aminopropylsilane groups. On the other hand, the ionene was prepared according to the literature procedure [23] and then the ionene was added to the nano particle prepared before. The last stage was supporting of perbromide on the core-shell ionene nano particle in acetic acid.

The characteristic advantages of this catalyst are rapid, simple and efficient separation by using an appropriate external magnet, which minimizes the loss of catalyst during separation, and are reusable without significant loss of activity up to 6 cycles.

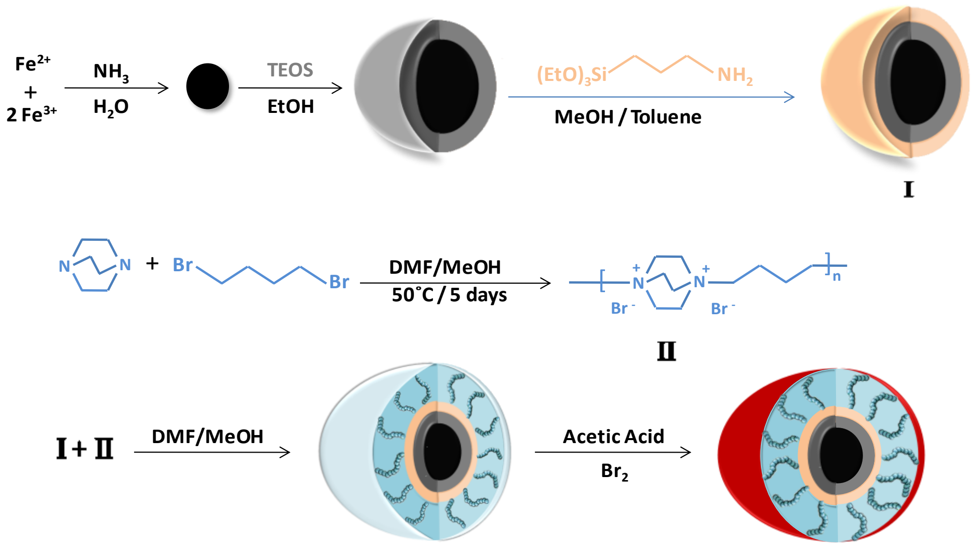

Scheme 1. Preparation of Fe_3O_4@SiO_2@polyionene/Br_3^- magnetic core-shell-shell catalyst.

2- Experimental

2-1 Materials and apparatus

All chemicals were purchased from Fluka and Merck and Sigma-Aldrich companies and used without further purification. Products were characterized by comparing their spectral (IR, 1HNMR, and TLC) and physical data (m.p and b.p) with those of authentic samples. Fourier transform infrared (FT-IR) spectra were obtained using a Shimadzu FT-IR 8400 spectrophotometer. 1HNMR spectra were recorded with a DPX-500 advance spectrometer (Bruker Corporation, MA,USA) at 500 MHz in $CDCl_3$ or DMSO-d_6 as the solvent and tetramethyl silane as internal reference. Melting points were measured with Electrothermal 9300 (Electrothermal, Essex, UK). Soltec Sonica Mod 3200 ETH ultrasonic cleaner bath (Soltec S.r.l, Milan, Italy) was used for ultrasonic irradiation. The reaction vessal placed inside the ultrasonic bath contained water. X-ray diffraction (XRD) patterns of samples were taken on a Panalytical X-ray diffractometer Model X□PertPro at 40 kV and 30 mA with Cu

Kα radiation (λ = 1.5418 A˚). The thermal stability was determined by Thermal Gravimetric and Differential Thermal Analysis (TG-DTA, Perkin Elmer Instruments model, Pyris 6) and Differential Scanning Calorimeter (DSC, Perkin Elmer Instruments model, Pyris diamond). The termograms were recorded for 5 mg of powder sample from room temperature to 550 ˚C at a heating rate of 10 ˚C/min under nitrogen atmosphere. Morphology and size of the nanoparticles was examined by a Philips XL30 scanning electron microscope (SEM) with gold coating and a Zeiss-EM10C-80KV transmission electron microscope (TEM). The nanoparticles were dispersed in deionized water, sonicated in an ultrasonic bath for 10 min, and then a droplet was deposited on a formvar carbon coated grid Cu Mesh 300. The nanoparticles were then allowed to dry prior to imaging. The magnetic properties were measured by a BHV-55 vibrating sample magnetometer (VSM). Magnetic separation was done by a super magnet with 1.4 Tesla magnetic fields.

2-2- Preparation of catalyst

2-2-1 preparation of polyionene

Typically, DABCO (15 mmol, 1.683 g) and 1,4-dibromobutane (15 mmol, 3.23 g) were dissolved in a mixture of DMF (25 mL) and MeOH (25 mL) at 50 ˚C under N_2 atmosphere and vigorous mechanical stirring for 5 days. The resulting white solid product was filtered, washed with acetone 10 mL and dried in vacuum desiccator over calcium chloride.

2-2-2- Preparation of magnetic nanoparticles (Fe_3O_4)

Magnetic nanoparticles (MNPs) precipitated in alkali solution of Fe(III) and Fe(II) (molar ratio 2:1) at 80 ˚C via the standard co-precipitation method reported by Liu et al. [26]. Typically, $FeCl_3.6H_2O$ (10 mmol, 2.7 g) and $FeSO_4.7H_2O$ (10 mmol, 1.39 g) were dissolved in 100 mL deoxygenated distilled water at 80 ˚C under N_2 protection and vigorous mechanical stirring. Then, 7.5 mL of ammonium hydroxide was quickly injected into the reaction mixture in one portion. The addition of the base to the Fe^{2+}/Fe^{3+} salt solution resulted in the formation of the black precipitate of MNPs immediately. The reaction continued for another 60 min and the mixture was cooled to room temperature. The resulting black precipitate was isolated via applying an external magnetic field and then washed four times with water followed by drying in vacuum at room temperature for 48 h.

2-2-3- Preparation of silica-coated MNPs (Fe_3O_4@SiO_2)

The core/shell Fe_3O_4@SiO_2 was prepared according to the Stober process [27] with some modifications. The obtained MNPs powder (1g) were dispersed in a mixture of 100 mL of ethanol, 20 mL of distilled water by the ultrasonic treatment for 30 min and 5.0 mL of 28 wt % concentrated ammonia aqueous solution ($NH_3.3H_2O$) with vigorous stirring, followed by the addition of 2 mL of TEOS was dropwise added to this dispersion. The resulting dispersion was kept stirred mechanically under N_2 protection for 12 h at room temperature. The obtained Fe_3O_4@SiO_2 nanoparticles were separated with a magnet and washed repeatedly with ethanol and water to remove nonomagnetic byproduct.

2-2-4- Preparation of amino propyl modified silica-coated magnetic nanoparticles (Fe_3O_4@SiO_2@APTES)

Then, the obtained MNP powder (1g) was dispersed in methanol (100 mL) and toluene (30 mL) by the ultrasonic treatment for 30 min before 3-aminopropyltriethoxysilane, APTES, (99%, 1 mL) was added to the mixture. After mechanically agitation for 12 h, the suspended substance was separated by a magnet. The settlement product was re-dispersed in ethanol by sonication and isolated with magnetic decantation for 5 times. The precipitated product (APTES-MNPs) was dried at room temperature under vacuum.

2-2-5- Preparation of tribromide modified silica-coated magnetic nanoparticles (Fe_3O_4@SiO_2@polyionene/Br_3^-)

After the Fe_3O_4@SiO_2@APTES (0.5g) was dispersed in DMF (30 mL) and MeOH (30 mL) by the ultrasonic treatment for 30 min. Then, ionene in the presence of $NaHCO_3$ (1mmol, 0.084 g) was added into the mixture under vigorous stirring for 3 days. The Fe_3O_4@SiO_2polyionene/Br^- was separated from the solution by magnetic decantation, and it was washed several times with acetone then dried. The Fe_3O_4@SiO_2@polyionene/Br^- (0.5g) was dispersed in acetic acid (10 mL) by the ultrasonic treatment for 30 min, molecular bromine (2 ml, 0.038 mol) was added dropwise for over 15 min to Fe_3O_4@SiO_2@polyionene/Br^- stirring and cooling in an ice-bath with stirring being continued for 2 h. The resulting dark orange solid was collected by magnetic and washed with 5 mL acetic acid.

2-3- General procedure for the synthesis of imidazoles derivatives

A mixture of aldehyde (1mmol), ethylene diamine (or ortho-phenylene diamine or 2-amino thiophenol or 1,8-diamino naphtalene or 2-amino phenol) (1mmol), and Fe_3O4@SiO_2@polyionene/Br_3^- MNPs (0.05 g) was mixed and the reaction was heated at 110˚C under solvent-free condition for appropriate time (table 3). After completion of the reaction as indicated by thin-layer chromatography (TLC), EtOH (10 mL) was added to the reaction mixture and the catalyst was recovered by an external magnet, and the reaction mixture was put into ice-water. The solid product was filtered, washed with water (20 mL) and diethyl ether (20 mL) and dried under vacuum to yield the product that was used without further purification. In the recycling experiment, the separated catalyst was washed with ethanol and dried under vacuum at room temperature to remove residual solvent. All the desired products were characterized by comparison of their physical and spectral data with those reported compounds.

Physical and spectral data for some representative imidazole, benzimidazole, benzothiazole, and perimidine derivatives

2-(4-Hydroxyphenyl)-1H-benzimidazole (Table 3, Entry 3): m.p. 262-265 ˚C (lit. 265-267 ˚C) [36]; ^{1}H NMR (200 MHz, DMSO-d_6): δ (ppm): 5.04 (br, 1H, OH), 6.91 (d, *J* = 8.7 Hz, 2H), 7.12-7.21 (m, 2H), 7.48-7.57 (m, 2H), 7.97 (d, *J* = 8.7 Hz, 2H), 10.02 (br, 1H, NH); ^{13}C NMR (50 MHz, DMSO-d_6): δ (ppm): 120.1, 121.4, 125.9, 127.6, 133.9, 144.2, 157.1, 165.0.

2-(p-Tolyl)-1H-benzimidazole (Table 3, Entry 4): m.p. 262-265 ˚C (lit. 264-265 ˚C)[34]; ^{1}H NMR (200 MHz, DMSO-d_6): δ (ppm): 2.57 (s, 3H), 7.14-7.20 (m, 2H), 7.34 (t, *J* = 8.0 Hz, 2H), 7.49 (t, *J* = 8.0 Hz, 1H), 7.62 (t, *J* = 8.0 Hz, 1H), 8.03-8.07 (m, 2H), 12.92 (br, 1H, NH); ^{13}C NMR (50 MHz, DMSO-d_6): δ (ppm): 21.3, 111.5, 119.1, 122.3, 127.3, 129.9, 135.3, 144.2, 151.7.

2-(4-Chlorophenyl)-1H-benzimidazole (Table 3, Entry 6): m.p. 288-290 ˚C (lit. 288-291 ˚C)[37]; ^{1}H NMR (200 MHz, DMSO-d_6): δ (ppm): 7.35-7.41 (m, 2H), 7.76-7.83 (m, 4H), 8.32-8.39 (m, 2H), 13.17 (br, 1H, NH); ^{13}C NMR (50 MHz, DMSO-d_6): δ (ppm): 111.9, 119.4, 122.3, 123.2, 128.6, 129.5, 135.2, 150.6.

2-Phenylbenzothiazole (Table 4, Entry 1): m.p. 111-112 ˚C (lit. 112-114 ˚C)[38]; ^{1}H NMR (200 MHz, DMSO-d_6): δ (ppm): 7.54–7.59 (m, 5H), 8.07-8.13 (m, 4H); ^{13}C NMR (50 MHz, DMSO-d_6): δ (ppm): 123.3, 123.8, 126.5, 127.6, 128.1, 130.3, 132.3, 133.7, 135.3, 154.4, 168.2.

2-(p-Tolyl)benzothiazole (Table 4, Entry 4) : m.p. 81-83 ˚C (lit. 85 ˚C)[39]; ^{1}H NMR (200 MHz, $CDCl_3$), δ (ppm): 2.40 (s, 3 H), 7.24-7.48 (m, 4 H), 7.85-8.03 (m, 4 H); ^{13}C NMR (50 MHz, $CDCl_3$), δ (ppm): 22.0, 122.0, 123.5, 125.4, 126.7, 127.9, 130.2, 131.3, 135.4, 141.9, 154.6, 168.7.

2-(p-Tolyl)-2,3-dihydro-1H-perimidine (Table 5, Entry 3): m.p. 162-164 ˚C (lit. 161-163 ˚C)[42]; IR (KBr): ν (Cm^{-1}): 3365, 3039, 2922, 1601, 1485, 1417; ^{1}H NMR (400 MHz, DMSO-d_6): δ (ppm): 2.35 (s, 3H, CH_3), 5.34 (s, 1H, CH), 6.49-7.51 (m, 12H, CH_{arom}, 2NH); ^{13}C NMR (100 MHz, DMSO-d_6): δ (ppm): 20.8, 66.6, 104.2, 112.4, 115.1, 126.8, 127.8, 128.7, 134.3, 137.7, 138.8, 143.1.

2-(3-Nitrophenyl)-2,3-dihydro-1H-perimidine (Table 5, Entry 5): m.p. 186-188 ˚C (lit. 188-190 ˚C)[42]; IR (KBr): ν (Cm^{-1}): 3344, 3226, 2821, 1606, 1529, 1415, 1333; ^{1}H NMR (400 MHz, DMSO-d_6): δ (ppm): 5.56 (s, 1H, CH), 6.52-8.45 (m, 12H, CH_{arom}, 2 NH); ^{13}C NMR (100 MHz, DMSO-d_6): δ (ppm): 64.8, 104.6, 112.4, 115.6, 122.6, 123.2, 126.9, 129.9, 134.2, 134.6, 142.2, 144.5, 147.6.

2-Phenyl-1H-imidazole (Table 6, Entry 1): m.p. 100-102 ˚C (lit. 101 ˚C)[44]; ^{1}H NMR (200 MHz, DMSO-d_6): δ (ppm): 7.19-7.23 (m, 2H), 7.51-7.61 (m, 5H), 8.16-8.21 (m, 2H), 12.91 (br, 1H, NH); ^{13}C NMR (50 MHz, DMSO-d_6): δ (ppm): 120.1, 123.2, 127.0, 127.3, 129.7, 130.7, 131.0, 152.1.

3- Results and discussion

3-1- Characterization of ionene and nanoparticle

The morphology and dimensions of nanoparticles were examined using a Scanning electron microscopy (Philips XL 30 SEM) and transmission electron microscopy (Zeiss-EM10C-80KV TEM). The particles were analyzed for phase composition using X-ray diffraction (XRD) on a diffractometer (Panalytical X’Pert Pro) using Cu-Kα radiation (λ = 1.54056A˚). In order to confirm the iron oxide phase, the nature of coating and its bonding on the surface, Fourier transform infrared spectra (FTIR) was recorded between 4000 and 400 cm^{-1} on a Bruker Advance DPX 500 MHz instrument spectrometer. Magnetic studies at room temperature carried out using a BHV-55 vibrating sample magnetometer (VSM). Finally, the thermal stability was determined by thermogravimetric analysis (TGA) coupled with differential thermal analysis (DTA) (Perkin Elmer Instruments model, Pyris 6) and differential scanning calorimetric (DSC) analysis (Perkin Elmer Instruments model, Pyris diamond).

3-1-1- SEM and TEM analysis

The prepared polyionene were characterized by SEM (Fig. 1). These images confirmed average diameter size of the ionene are less than 20 nm.

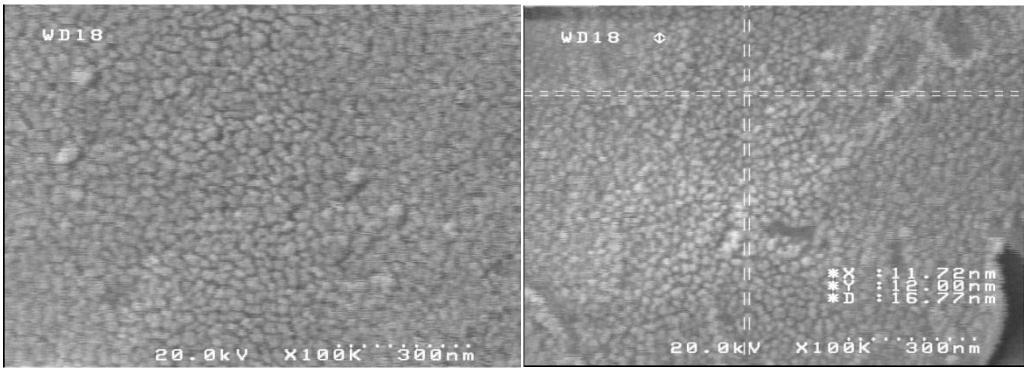

Fig.1. SEM images of prepared ionene

Scanning electron microscopy (SEM) is a useful tool to determine the size and morphology of the prepared catalyst. As shown in the images Fig. 2, nanoparticles in all the samples have a spherical shape indicating the nanocatalyst has a large surface area. The SEM image of the silica-supported MNPs showed that the particle size distribution is about 20 nm which indicate silica is successfully anchoring to the magnetic particles (Fig. 2a). Also, SEM observation showed that Fe_3O_4@SiO_2@Polyionene/Br_3^- MNPs have the average size less than 50 nm (Fig. 2c).

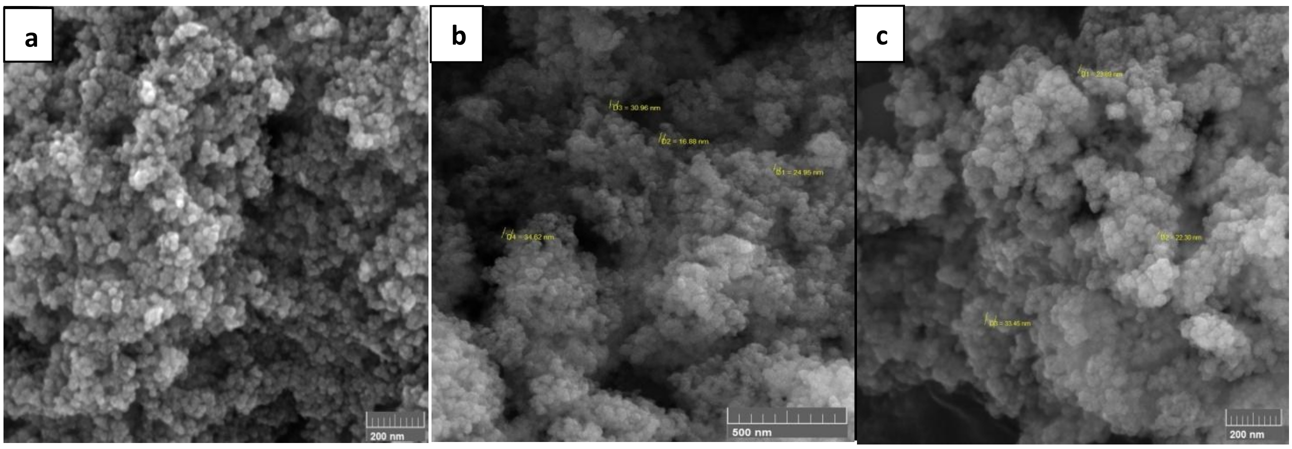

Fig.2. SEM images of (a) Fe_3O_4@SiO_2@APTES (b) Fe_3O_4@SiO_2@Polyionene/Br^- (c) Fe_3O_4@SiO_2@polyionene/Br_3^-.

The size and morphology of the prepared catalyst were characterized by TEM (Fig. 3). According to Fig. 3, Fe_3O_4 nanoparticles have spherical shapes with nano dimension ranging from 12-15 nm. As shown in Fig. 3, the nanoparticles depicted varied spherical sizes. The TEM (Fig. 3a) observation indicates that TEOS coated Fe_3O_4 MNPs have average diameter ranging about 20 nm. The silica-modification process of MNPs leads to the formation of a core-shell structure and confirms the formation of a silica layer with thickness about 5 nm around the Fe_3O_4 nanoparticles. The TEM (Fig. 3b) observation of Fe_3O_4@SiO_2@APTES exhibit recognizable layers in magnetic nanoparticles. The thickness of polyionene layer is estimated about 8 nm (Fig. 3c). $Fe_3O_4@SiO_2@Polyionene/Br_3^-$ nanocatalyst has a typical core-shell-shell structure with average size of less than 50 nm (Fig. 3c).

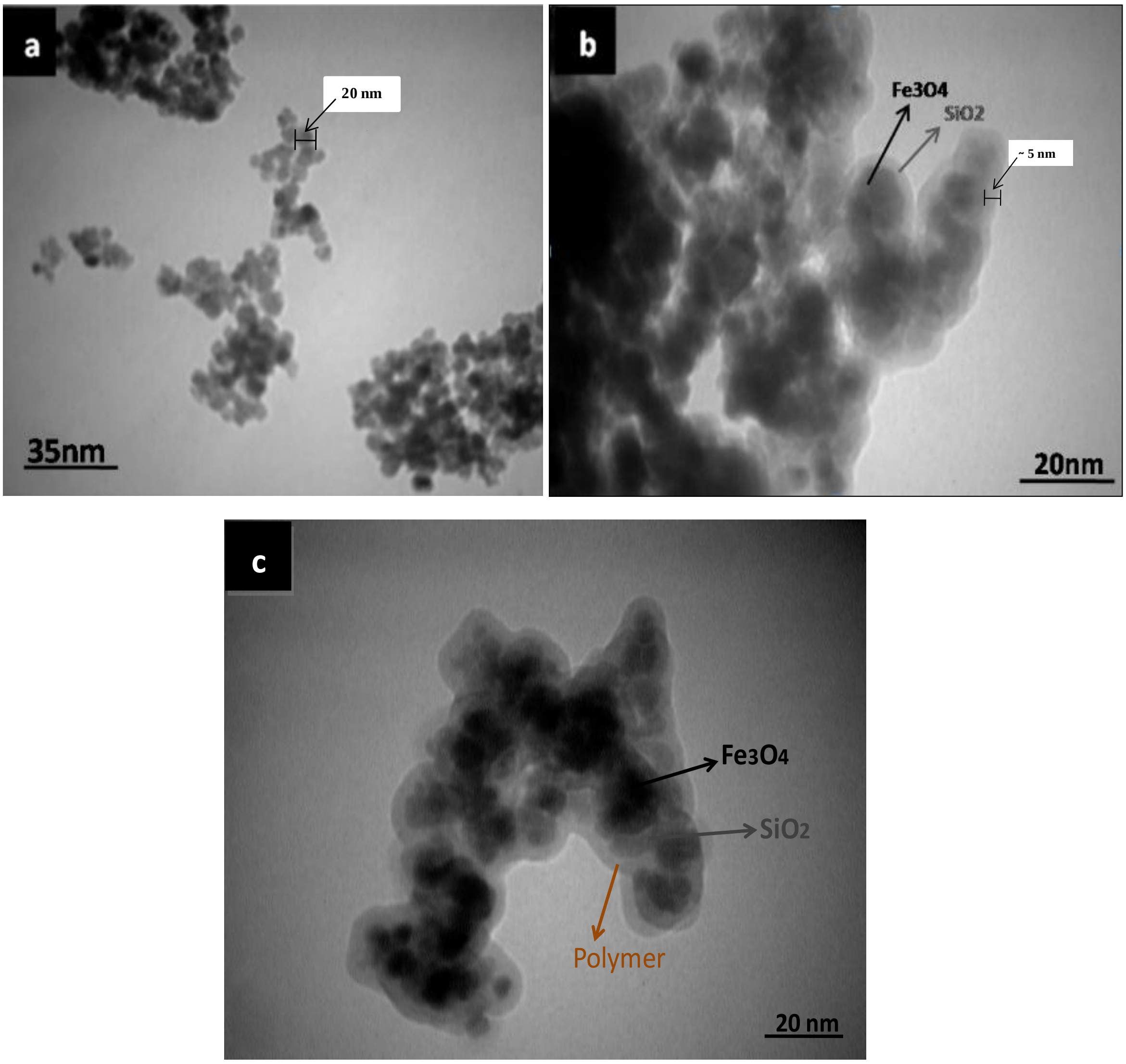

Fig.3. TEM images of (a) $Fe_3O_4@SiO_2$ (b) APTES coated Fe_3O_4 MNPs (c) $Fe_3O_4@SiO_2@Polyionene/Br_3^-$.

3-1-2- X-ray diffraction analysis

The crystalline structures of the Fe_3O_4 particles, $Fe_3O_4@SiO_2$, APTES coated Fe_3O_4 MNPs and $Fe_3O_4@SiO_2@Polyionene/Br_3^-$ were determined by powder X-ray diffraction (XRD) (fig. 4 a-d). As shown in fig. 4, the obtained Fe_3O_4 has crystalline cubic spinel structure which agrees with the standard Fe_3O_4 XRD spectrum. According to the database of Joint Committee on Powder Diffraction Standards (JCPDS No. 19–0629), the XRD pattern of a standard Fe_3O_4 crystal with cubic structure has six characteristic peaks at $2\theta = 30.4^\circ$, 35.8°, 43.6°, 53.7°, 57.5°, and 63.2° [28]. The pattern of $Fe_3O_4@SiO_2@Polyionene/Br_3^-$ displays the most intense peak at $2\theta = 35.80^\circ$ which is completely corresponded to the pure Fe_3O_4 and confirms the presence of Fe_3O_4 [29]. Therefore, it is concluded that the prepared $Fe_3O_4@SiO_2@Polyionene/Br_3^-$ show spinel structure and these modifications don't cause a phase change in Fe_3O_4.

The highest intensity peak (311) of the particles was picked out to evaluate D (average crystalline diameter) according to the Debye-Scherrer equation: $D = k\lambda/(\beta\cos\theta)$, where θ is the Bragg's angle in degrees, λ is the X-ray wavelenght in 1.5418 A°, β is the corrected width of the XRD 311 peak at half-height and k is the scherrer constant ($k = 0.94$) [30]. The average particle size obtained from XRD data found to be 49.17 nm. This value is close to the mean particle size observed from TEM images.

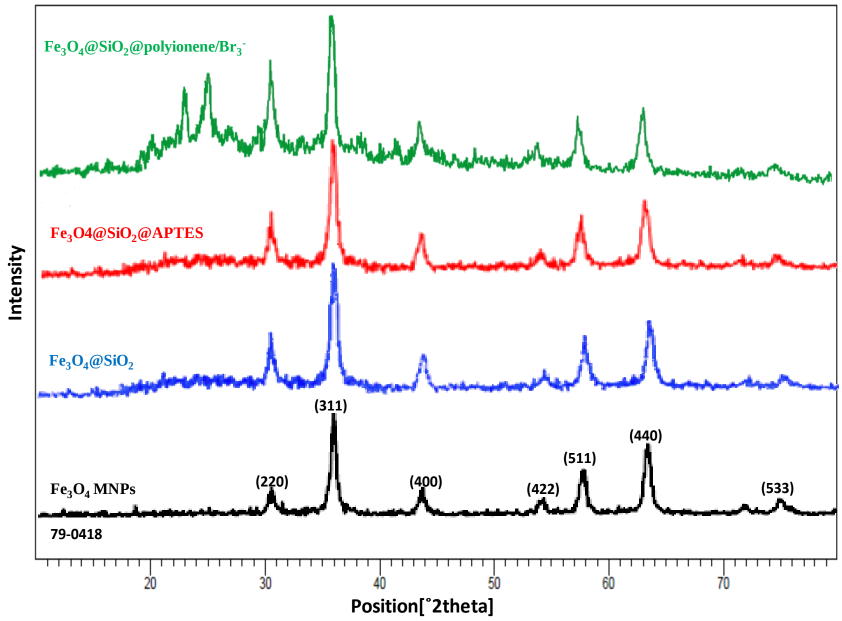

Fig.4. XRD patterns of (a) Fe_3O_4 MNPs; (b) Silica coated Fe_3O_4 MNPs; (c) APTES coated Fe_3O_4 MNPs and (d) $Fe_3O_4@SiO_2@polyionene/Br_3^-$

3-1-3- FTIR spectroscopy

The FTIR spectra of bare MNPs, Fe_3O_4@SiO_2 MNPs, Fe_3O_4@SiO_2@APTES MNPs and Fe_3O_4@SiO_2@Polyionene/Br_3^- MNPs are presented in Fig.5. The signal observed at 585 cm^{-1} is attributed to the presence of Fe-O stereching vibration [31]. The broad band at 3300–3500 cm^{-1} is due to -OH stretching vibrations (Fig. 5a). The adsorption of silane polymer onto the surface of magnetite particles was confirmed by bands at 951, 804 and 1086 cm^{-1} which correspond to the Si-OH and Si–O–Si groups (Fig. 5b). Characteristic Fe-O peak of bare MNPs at 585 cm^{-1} is shifted to 580 and 578 cm^{-1} in the spectrum of Fe_3O_4/SiO_2 MNPs and Fe_3O_4@SiO_2@APTES MNPs, respectively. Thus, undoubtedly it can be said that the silica shell is linked to the surface of the magnetic nanoparticles by Fe-O-Si chemical bond [32]. Compared with MNP, APTES-MNP presents absorption bands at 2958 and 2854 cm^{-1} assigned to stretching vibration of C–H bond of the propyl amine group, which prove successful grafting of APTES on silica coated magnetic particles. The two broad bands at 1628 and 3435 cm^{-1} are attributed to the N–H stretching vibrations and bending mode of free $–NH_2$ group, respectively (Fig. 5c). These results illustrate that MNs are coated by SiO_2 and APTES. Fe_3O_4@SiO_2@Polyionene/Br_3^- showed a band at 1448 cm^{-1} which is characteristic for the tertiary amine group in backbone of ionene (Fig. 5d).

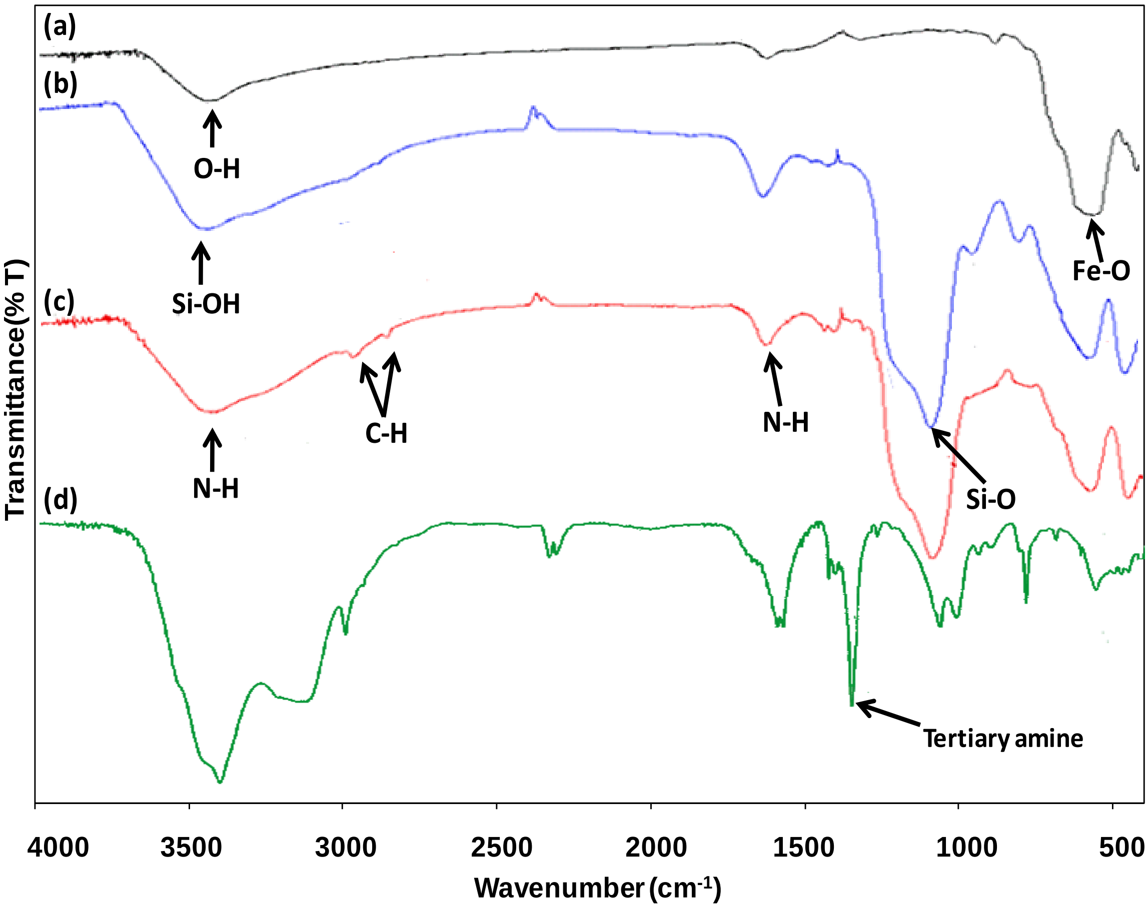

Fig.5. FT-IR spectra of (a) Fe_3O_4 MNPs; (b) Silica coated Fe_3O_4 MNPs; (c) APTES coated Fe_3O_4 MNPs and (d) $Fe_3O_4@SiO_2@Polyionene/Br_3^-$.

3-1-4- Magnetic properties of nano catalyst

The magnetic properties of Fe_3O_4 MNPs were characterized by vibrating sample magnetometer (VSM). Fig. 6 shows the typical room temperature magnetization curves of bare Fe_3O_4 MNPs (Fig. 6a), Silica coated Fe_3O_4 MNPs (Fig. 6b), APTES coated Fe_3O_4 MNPs (Fig. 6c), and $Fe_3O_4@SiO_2@Polyionene/Br_3^-$ (Fig. 6d), respectively. All of the samples show a typical superparamagnetic behavior. However, the saturation magnetization of the nanoparticles is 70.0 emu/g (Fig.6a), which is lower than its bulk counter parts (92.0 emu/g) [33]. The saturation magnetization of $Fe_3O_4@SiO_2@polyionene/Br_3^-$ MNPs was 10.0 emu/g of particles, which is lower than that of bare magnetic nanoparticles. This might result from the formation of a silica shell and polyionene shell as double layer around the Fe_3O_4 core.

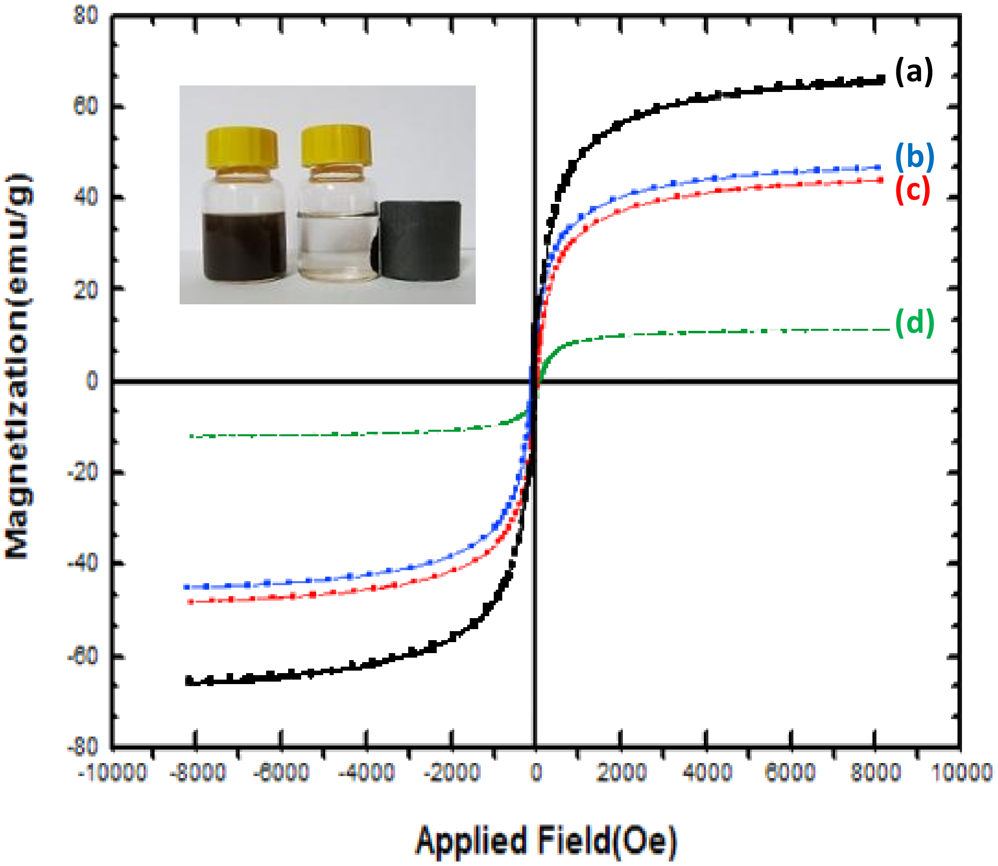

Fig.6. Magnetization curves obtained by VSM at room temperature of (a) Fe_3O_4 MNPs; (b) Silica coated Fe_3O_4 MNPs; (c) APTES coated Fe_3O_4 MNPs and (d) Fe_3O_4@SiO_2@polyionene/Br_3^-

The thermal stability of Fe_3O_4@SiO_2@Polyionene/Br_3^- nano particles was analyzed by TGA, DTA and DTG. The thermogravimetric analysis (TGA) thermogram of Fe_3O_4@SiO_2@Polyionene/Br_3^- catalyst is presented in fig. 8. As was observed from the curve, the sample shows a three-step degration pattern in the temperature range of 30-500 ˚C. The initial weight loss up to 100 ˚C is due to the removal of the adsorbed water and surface hydroxyl groups of the catalyst. Two steps of the another weight loss about 50 % in the region of 250-500 ˚C is the result from the termal decomposition of organic materials grafting to the MNPs surface (fig. 8). The differential thermogravimetric analyzer (DTG) also exhibit a sharp peak at 277.5 ˚C and the another peak at 338.4 ˚C due to the breakdown and decomposition of organic moieties. The corresponding result was obtained by the DTA (fig. 8). On the basis of this results, the well grafting of polyionene on the MNPs is verified.

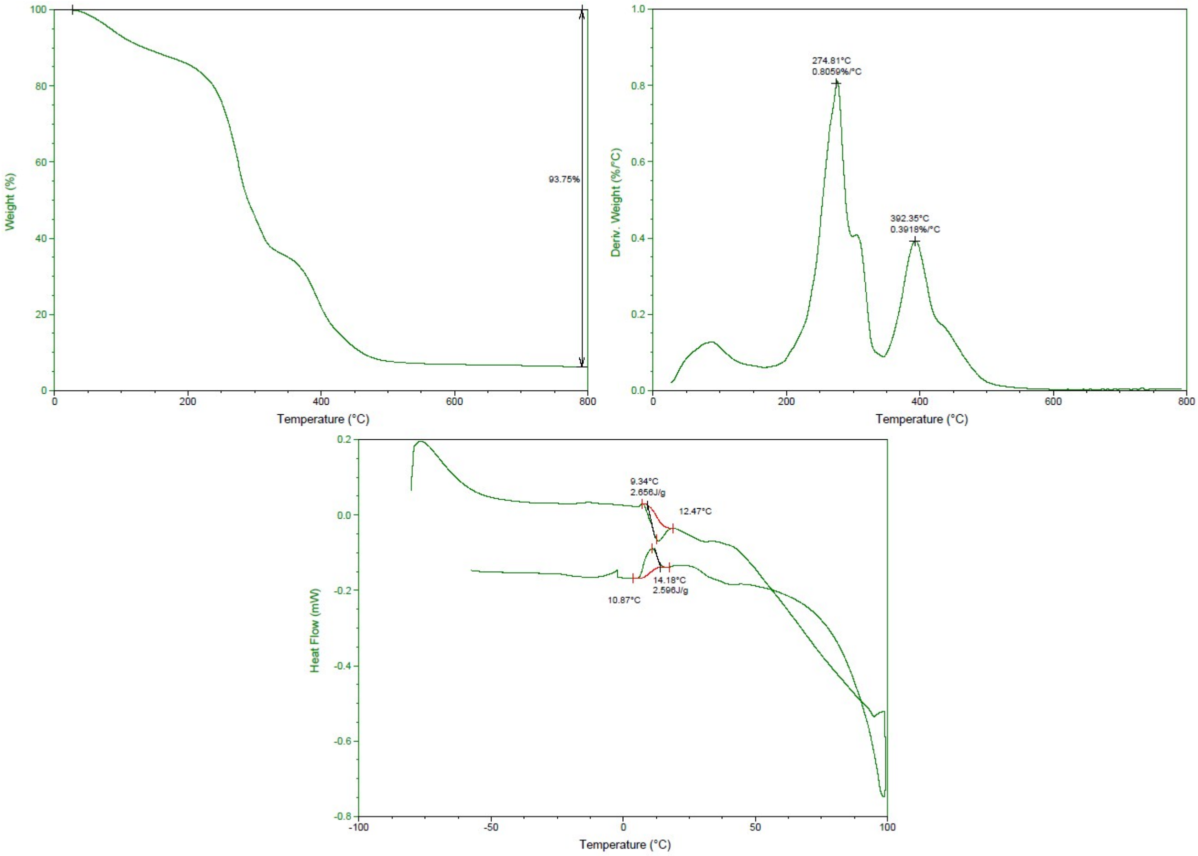

Fig.7. TGA and DSC curves of polyionene

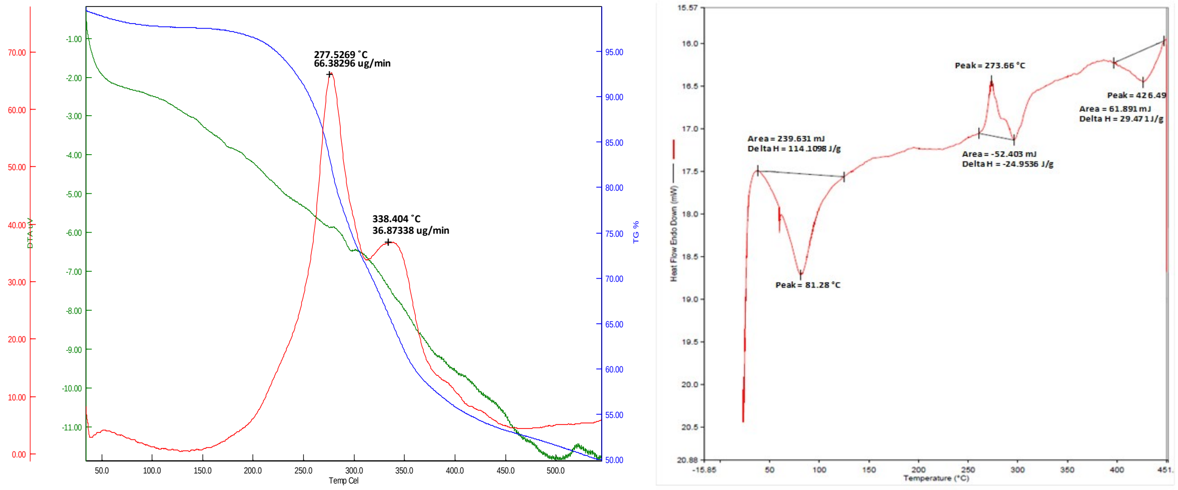

Fig.8. TGA and DSC curves of Fe_3O_4@SiO_2@polyionene/Br_3^-

3-2- Catalyst application of Fe_3O_4@SiO_2@polyionene/Br_3^- for synthesis of imidazole derivatives

The developed methodology is simple and proceeded in high to excelent yields. We first compared the catalyst effect on different solvents for synthesis of imidazole derivatives using this reagent. The results are summarized in table 1.

Table 1. Optimization of reaction conditions for the synthesis of 2-(4-chlorophenyl)-1*H*- benzimidazole

Entry	Solvent [a]	Time (min)	Yield (%)
1	CH_3CH_2OH	60	34
2	CH_2Cl_2	60	<10
3	$CHCl_3$	60	<10
4	CH_3CN	60	21
5	THF	60	trace
6	Toluene	60	trace
7	DMF	60	trace
8	None [b]	60	64
9	None [c]	60	89
10	None [d]	15	94

The reactions were performed with 4-chloro benzaldehyde (1mmol), ortho-phenylene diamine (1mmol), and catalyst (0.05 g) under different reaction conditions. a) reflux condition, b) in solvent- free condition at 50˚C, c) in solvent- free condition at 80˚C, d) in solvent- free condition at 110˚C

In a typical experiment, the reaction was carried in solvent or solvent-free conditions in the presence of Fe_3O_4@SiO_2@polyionene/Br_3^- to afford the corresponding imidazoles (or thiazoles). We used different solvents like ethanol, dichloro methane, chloroform, acetonitrile, toluene, THF and DMF. In all cases, the experimental results show that the yields of the products are trace.

Furthermore, the effect of catalyst load on reaction time and yield is explored in table 2. Using lower amount of catalyst resulted in lower yields, while higher amount of catalyst did not affect the reaction times and yields, and in the absence of catalyst, the yield of the product was not found. The best results were obtained using 0.05 g of the catalyst (table 2, entry 2). Based on the results of this study, it seems that the reaction times and yields will improve in the solvent-free conditions at 110 ˚C.

Table 2. Effect of increasing amount of catalyst on the preparation of 2-(4-chlorophenyl)-1*H*-benzimidazole

Entry	Amount of catalyst(g)	Time (min)	Yield (%)
1	0.025	45	81
2	0.05	15	94
3	0.075	15	94
4	0.1	15	91
5	None	60	trace

The reactions were performed with 4-chloro benzaldehyde (1mmol), ortho-phenylene diamine (1mmol), and different amounts of catalyst under solvent-free conditions at 110 ˚C.

After optimizing the conditions, the generality of this method was examined by the reaction of several substituted aldehydes with some 1,2-diamine and 1-amino-2-mercapto derivative compounds. The results are shown in tables 3-6. The products were isolated and identified by melting point, 1HNMR, and IR.

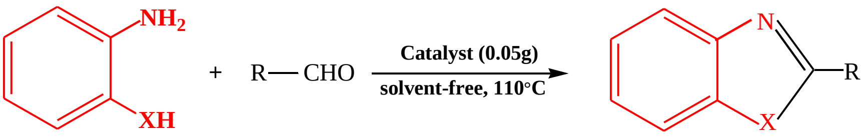

R = alkyl, aryl X = NH, O

Table 3. Synthesis of benzimidazole derivatives and benzoxazole catalyzed by $Fe_3O_4@SiO_2@polyionene/Br_3^-$ under solvent-free conditions at 110 °C

Entry	R	X	Product	Time (min)	Yield (%)	MP (°C)	
						Found	Reported[ref]
1	C_6H_5	NH	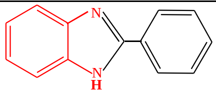	15	93	290-291	290-293[34]
2	$4\text{-}OMeC_6H_4$	NH	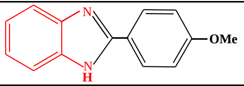	12	97	225-226	223-226[35]
3	$4\text{-}OHC_6H_4$	NH	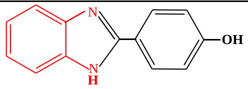	13	88.5	262-265	265-267[36]
4	$4\text{-}MeC_6H_4$	NH	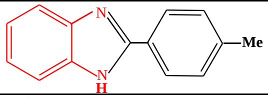	12	91	262-265	264-265[34]
5	$4\text{-}NO_2C_6H_4$	NH	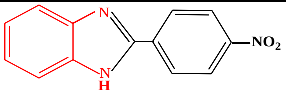	25	98	319-321	322-323[34]
6	$4\text{-}ClC_6H_4$	NH	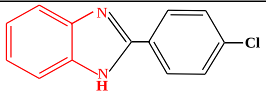	15	94	288-290	288-291[37]
7	3-Phenyl propyl	NH	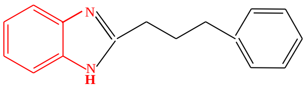	90	67		
8	$4\text{-}ClC_6H_4$	O	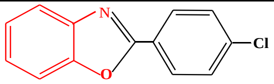	–	No reaction	–	

using an aliphatic aldehyde instead of aromatic one produces benzimidazole in lower yield and longer time. In contrast, if the 2-amino phenol is used, any heterocyclic products to be seen (table 3, entry 7,8).

When 2-amino thiophenol was used instead of *ortho*-phenylene diamine, the aldehydes reacted in more convenient condition and the yields were higher (table 4).

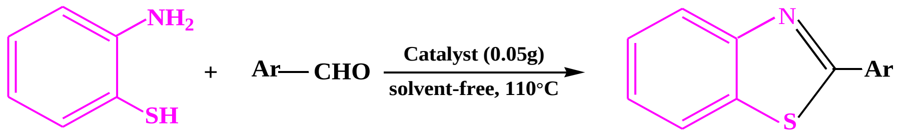

Table 4. Synthesis of benzthiazole derivatives catalyzed by $Fe_3O_4@SiO_2@polyionene/Br_3^-$ under solvent-free conditions at 110 ˚C

Entry	Ar	Product	Time (min)	Yield (%)	MP (˚C) Found	MP (˚C) Reported[ref]
1	C_6H_5	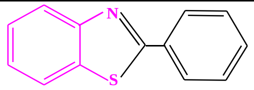	15	95	111-112	112-114[38]
2	$4\text{-}OHC_6H_4$	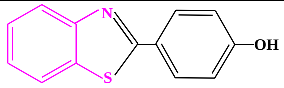	10	94	225-226	227[39]
3	$4\text{-}OMeC_6H_4$	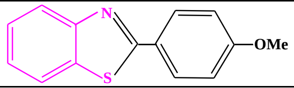	12	96	120-121	120-121[38]
4	$4\text{-}MeC_6H_4$	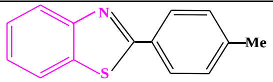	17	92	81-83	85[39]
5	$4\text{-}NO_2C_6H_4$	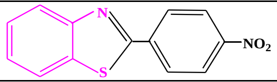	20	93	229-232	230-231[39]
6	$4\text{-}ClC_6H_4$	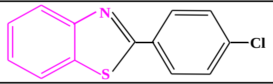	17	89	100-102	103-104[40]
7	$4\text{-}BrC_6H_4$	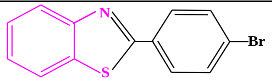	17	87	101-102	102-104[41]

Some aromatic aldehydes have reacted with 1,8-diamino naphthalene in the presence of MNs catalyst. As it is seen, the yields are higher than before. isolation of crude products are easy and recrytalization could be used for more purity (table 5).

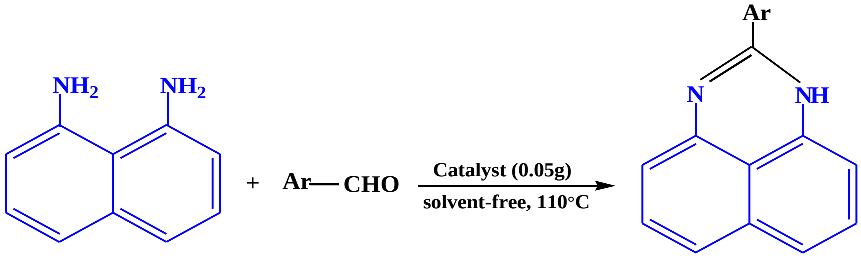

Table 5. Synthesis of perimidine derivatives catalyzed by $Fe_3O_4@SiO_2@polyionene/Br_3^-$ under solvent-free conditions at 110 ˚C

Entry	Ar	Product	Time (min)	Yield (%)	MP (˚C) Found	MP (˚C) eported[ref]

1	C_6H_5	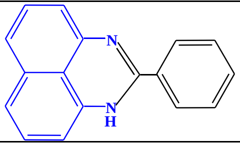	10	94	100-102	101-103[42]
2	$4\text{-}OHC_6H_4$	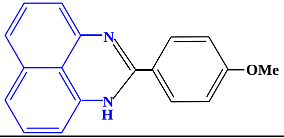	6	95	161-164	161-163[42]
3	$4\text{-}MeC_6H_4$	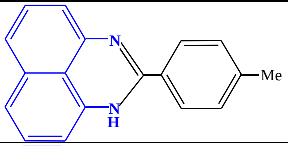	10	92	162-164	161-163[42]
4	$4\text{-}NO_2C_6H_4$	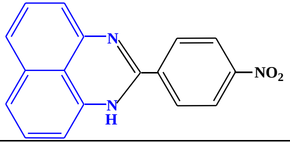	20	95	199-200	198-200[43]
5	$3\text{-}NO_2C_6H_4$	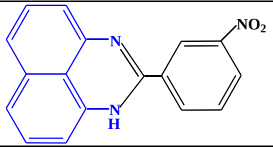	20	89	186-188	188-190[42]
6	$4\text{-}ClC_6H_4$	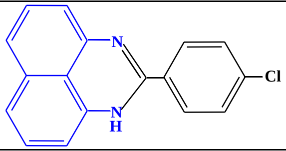	12	91	157-160	158-160[42]

Likewise, the reaction of ethylene diamine was carried out in solvent free condition. The product yields were lower than benzimidazoles due to evaporating of ethylene diamine in amidst of reaction (table 6).

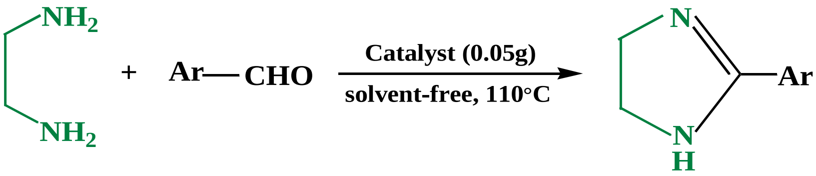

Table 6. Synthesis of imidazole derivative catalyzed by Fe_3O_4@SiO_2@polyionene/Br_3^- under solvent-free conditions at 110 ˚C

Entry	Ar	Product	Time (min)	Yield (%)	MP (˚C)	
					Found	Reported[ref]
1	C_6H_5	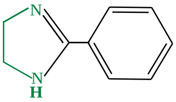	15	91	100-102	101[44]
2	$4\text{-}OHC_6H_4$	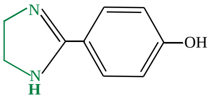	10	90		

3	4-OMeC$_6$H$_4$	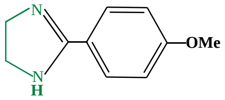	10	93	137-138 137-139[45]
4	4-MeC$_6$H$_4$	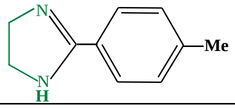	13	91	180-181 181-183[44]
5	4-NO$_2$C$_6$H$_4$	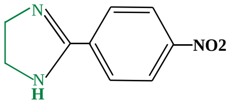	17	93	233-236 231[46]
6	4-ClC$_6$H$_4$	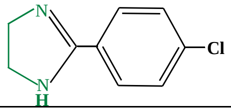	13	89	
7	4-BrC$_6$H$_4$	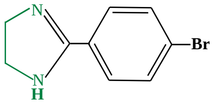	15	92	243-245 242-246[46]

Tables 3-6 shows some examples for this convenient procedure in high to excellent yields. In order to test this procedure for preparative scale applications, a variety of benzaldehydes bearing electron donating and electron-withdrawing substituents were successfully employed to prepare the corresponding imidazole derivatives in excellent yields.

We proposed a possible mechanism for the synthesis of 2-phenyl-1H-benzimidazole in the presence of Fe$_3$O$_4$@SiO$_2$@Polyionene/Br$_3^-$ as a model reaction, indicated in Scheme 2. The activation of the oxygen of carbonyl are tacke placed by the catalyst. Then, intramolecular attack are occuared by the second amino group to form a five-membere ring of 2-phenyl-2,3-dihydro-1H-benzo[d]imidazole **(b)**. The intermediate **b** then undergoes subsequent oxidation to give the desired benzimidazole as the final product.

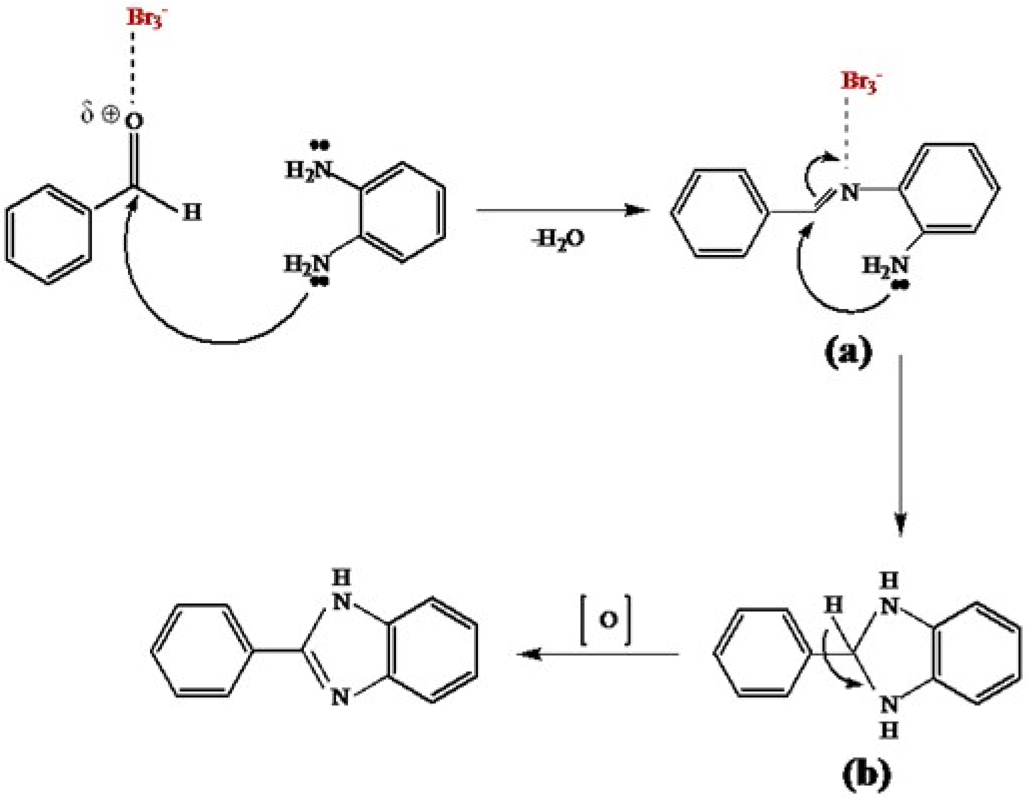

Scheme 2. Plausible mechanism for the synthesis of benzimidazole derivatives via condensation reaction of *o*-phenylenediamine with aryl aldehydes

The efficiency and applicability of $Fe_3O_4@SiO_2@Polyionene/Br_3^-$ nanocatalyst was compared with some recently reported catalysts in terms of percentage yield and reaction time for the preparation of 2-phenyl-1H-benzimidazole as a model reaction (table 7).

Table 7. Comparative study on the present method with the reported method

Entry	catalyst	conditions	Time (min)	Yield (%)^a [ref]
1	$Fe_3O_4@SiO_2@Polyionene/Br_3^-$ (0.05 g)	Solvent-free/ 110 ˚C	15	93 [this work]
2	Nano In_2O_3 (5 mol%)	CH_3CN/ 60 ˚C	120	89 [47]
3	$MgCl_2$. $6H_2O$ (10 mol%)	DMF/ 60 ˚C	100	93[48]
4	Indion-190 resin (10 mol%)	EtOH/ 70 ˚C	240	89[49]
5	NH_4OAc (1mmol)	EtOH/ 75 ˚C	270	95[50]
6	$Sm(OTf)_3$ (10 mol%)	CH_3CN/ r.t	240	90[51]
7	Scolecite acid (3 wt%)	EtOH/ 70 ˚C	55	89[52]

8	I_2 (1 mmol) /KI (25 mol%) /K_2CO_3 (1.5 mmol)	H_2O/ 90 ˚C	45	75[46]

[a] The reactions were performed with benzaldehyde (1mmol), ortho-phenylene diamine (1mmol) under different conditions.

3-3- Catalyst recovery

Recyclability of this nano magnetic catalyst was investigated in the reation between 4-chloro benzaldehyde and ortho-phenylene diamine. The catalyst was found to be reusable six times without significant loss of activity (Fig. 9). After completion of the reaction, ethanol was added to the reaction mixture which was then decanted using a external magnet. Nanoparticle was washed with ethanol and dried at 60 ˚C for 2 h. The recycled catalyst was used for 6 times with little loss of activity (Fig. 9).

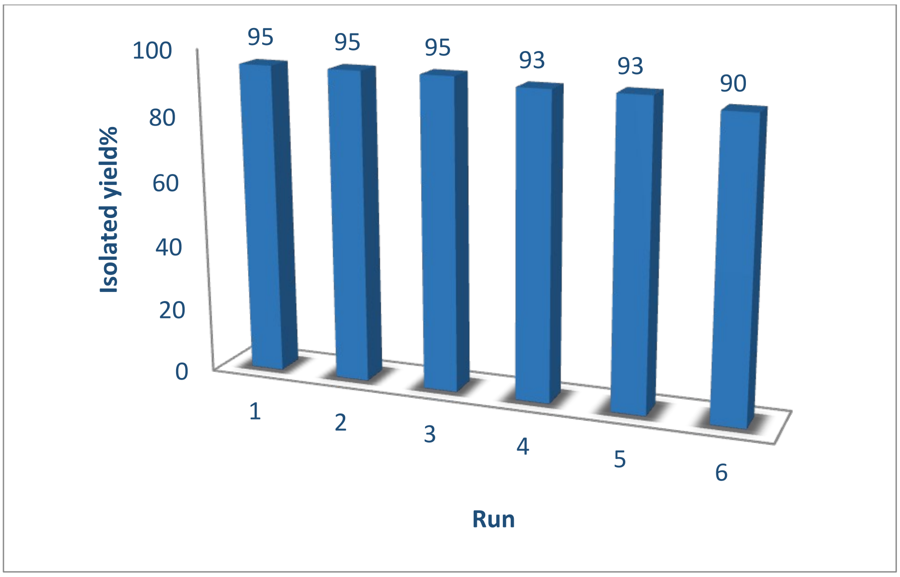

Fig. 9. Reuse of catalyst in synthesis of 2-(4-Chlorophenyl)-1H-benzimidazole

3-4- Catalyst stability

Fe_3O_4@SiO_2@polyionene/Br_3^- as a magnetic nanocatalyst showed a good shelf life for months. It can be stored as powder in room temperature. It did not show any loss of activity when compared with that of the freshly prepared reagent.

4- Conclusions

In this study, an efficient, and green method has been developed for synthesis of imidazole and thiazoles derivatives using novel magnetite nanoparticles Fe_3O_4@SiO_2@polyionene/Br_3^- as an efficient and recyclable catalyst. The prominent features of this method are short reaction time, simple workup procedure and high yield. In the presence of this catalyst, benzimidazole derivatives were produced in excellent yields (88.5-98 %) and low reaction time (12-25 min). using an aliphatic aldehyde instead of aromatic one, although in low yield and longer reaction time, was led to the corresponding benzimidazole. As well as, we replaced 2-amino thiophenol with *ortho*-phenylene diamine. Furtunately, the reactions were run in the shorter time (10-20 min) and high yields were obtained (87-96 %). Extension of this procedure to 1,8-diamino naphthalene were also examined and satisfactory yields (89-95 %) and low reaction time (6-20 min) were obtained. Finally, ethylene diamine was used with success to provide the corresponding imidazole derivatives in good yields (89-93 %) and in the time range of 10-17 min. In all of these reactions, the catalyst could be easily isolated using external magnetic field and recovered for 6 times without significant loss of activity.

Acknowledgment

Financial support from the Islamic Azad University of Kermanshah is gratefully acknowledged.

References

[1] (a) C.O. Dalaigh, S.A. Corr, Y.G. Ko, S.J. Connon, *Angewandte Chemie International Edition* **46** (2007) 4329-4332. (b) C. Brechignac, P. Houdy, M. Lahmani, editors. Nanomaterials and Nanochemistry. Springer-Verlag Berlin Heidelberg 2007.

[2] (a) A. Schatz, O. Reiser, W.J Stark, *Chemistry-A European Journal* **16** (2010) 8950-8967; (b) A.H. Lu, E.L. Salabas, F. Schuth, *Angewandte Chemie International Edition* **46** (2007) 1222-1244.

[3] V. Polshettiwar, R.S. Varma, *Organic & Biomolecular Chemistry* **7** (2009) 37-40.

[4] J. Zhang, Y. Wang, H. Ji, Y. Wei, N. Wu, B. Zuo, Q. Wang, *Journal of Catalysis* **229** (2005) 114-118.

[5] B. Panella, A. Vargas, A. Baiker, *Journal of Catalysis* **261** (2009) 88-93.

[6] H. Wang, Y. Zhang, F. Zhang, J. Niu, H. Yang, R. Li, J. Ma, *Solid State Sciences* **14** (2012) 1256.

[7] Y. Sun, G. Liu, H. Gu, T. Huang, Y. Zhang, H. Li, *Chemical Communications* **47** (2011) 2583-2585.

[8] B. Baruwati, D. Guin, S.V. Manorama, *Organic Letters* **9** (2007) 5377-5380.

[9] F. Zhang, J. Jin, X. Zhong, S. Li, J. Niu, R. Li, J. Ma, *Green Chemistry* **13** (2011) 1238-1243.

[10] J. Jung, A. Taher, Sh. Hossain, M. Jin, *Bulletin of the Korean Chemical Society* **31** (2010) 3010.

[11] S. Ceylan, C. Friese, C. Lammel, K. Mazac, A. Kirschning, *Angewandte Chemie International Edition* **47** (2008) 9134-9137.

[12] K. Fujita, S. Umeki, M. Yamazaki, T. Ainoya, T. Tsuchimoto, H. Yasuda, *Tetrahedron Letters* **52** (2011) 3137-3140.

[13] S. Luo, X. Zheng, J.P. Cheng, *Chemical Communications* **44** (2008) 5719-5721.

[14] V. Polshettiwar, R.S. Varma, *Chemistry-A European Journal* **15** (2009) 1582-1586.

[15] A. Farrokhi, K. Ghodrati, I. Yavari, *Cat. Commun* **63 (**2015) 41-46.

[16] A. U.S. Rembaum, Patent 4 046 750, 1977; Chem. Abstr. 1977;87: 152906j.

[17] K.H. Streun, P. Piet, A.L. German. *Eur Polym J* **23** (1987) 941-946.

[18] Y. Suzuki, F.H. Quina, A. Berthod, R.W. Williams, M. Culha, I.U. Mohammadzai, W.L. Hinze, *Anal Chem* **73** (2001) 1754-1765.

[19] J. Nagaya, A. Minakata, A. Tanioka, *Langmuir* **15** (1999) 4129-4134.

[20] W.H. Meyer, L. Dominguez, vol. **2**. In: J.R. MacCallum, C.A. Vincent, editors. Polymer electrolyte reviews. London: *Elsevier Applied Science*; 1989. p. 1987-1989.

[21] A.V. Pirogov, M.M. Platonov, O.A. Shpigun, *J Chromatogr* **850** (1999) 53-63.

[22] H. Noguchi, Y. Uchida, A. Nomura, Sh. Mori, *Journal of Materials Science Letters* **8** (1989) 1278-1280.

[23] M. M. Lakouraj, M. Tajbakhsh, F. Ramzanian-Lehmali, K. Ghodrati, *Monatsh. Chem* **139** (2008) 537–541.

[24] (a) D.A. Horton, G.T. Bourne, M.L. Smythe, *Chemical Reviews* **103** (2003) 893-930; (b) W.A. Denny, G.W. Rewcastle, B.C. Baugley, *Journal of Medicine Chemistry* **33** (1990) 814-819; (c) R. Cedillo-Rivera, O. Munoz, *Journal of Medical Microbiology* **37** (1992) 221-224; (d) G. Navarrete-Vazquez, R.Cedillo, A. Hernandez-Campos, L.Yepez, F. Hernandez-Luis, J. Valdez, R. Morales, R. Cortes, M. Hernandez, R. Castillo, *Bioorganic & Medicinal Chemistry Letters* **11** (2001) 187-190; (e) X. Bu,L. W.Deady, G. J. Finlay, B. C. Baguley, W.A. Denny, *Journal of Medicine Chemistry* **44** (2001) 2004-2014.

[25] (a) K. Bahrami, M.M. Khodaei, F. Naali, *Journal of Organic Chemistry* **73** (2008) 6835-6837. (b) A. Loupy, A. Petit, J. Hamelin, *Synthesis* **9**(1998) 1213-1234. (c) I. Bhatnagar, M.V. George, *Tetrahedron* **24** (1968) 1293-1298. (d) P.L. Beaulieu, B. Hache, E. von moos stanislaus (2003) 1683-1692. (e) M.A. Weidner-Wells, K.A. Ohemeng, V. N. Nguyen, S. Fraga-Spano, M.J. Macielag, H.M. Werblood, B.D. Foleno, G.C. Webb, J.F. Barrett, D. Hlasta, *Journal Bioorganic Medicine Chemistry Letters* **11** (2001) 1545-1548. (f) H. Fujioka, K. Murai, Y. Ohab, A. Hiramatsu, Y. Kita, *Tetrahedron Letters* **46** (2005) 2197. (g) M. Zendehdel, A. Mobinikhaledi, H. Alikhani, N. Jafari, *Journal of the Chinese Chemical Society* **57** (2010) 683-689.

[26] X. Liu, Z. Ma, J. Xing, H. Liu, *Journal of Magnetism and Magnetic Materials* **270** (2004) 1-6.

[27] W. Stober, A. Fink, E. J. Bohn, Journal of Colloid and Interface Science **26** (1968) 62-69.

[28] Y. Lin, H. Chen, K. Lin, B. Chen, C. Chiou, *J. Environ. Sci.* **23** (2011) 44–50.

[29] E.V. Stoyanov, I.C. Ivanov, D. Heber, *Molecules* **5** (2000) 19–32.

[30] S.R. Stock, B.D. Cullity, Elements of X-ray Diffraction, 3rd ed., Prentice-Hall, Englewood Cliffs, 2001, pp 167-171.

[31] R.D. Waldron, *Physical Review* **99** (1955) 1727-1735.

[32] F.H. Chen, Q. Gao, J.Z. Ni, *Nanotechnology* **19** (2008) 165103-165111.

[33] V.S. Zaitsev, D.S. Filimonov, I.A. Presnyakov, R.J. Gambino, B. Chu, *Journal of Colloid and InterfaceScience* **212** (1999) 49-57.

[34] K. Bougrin, A. Loupy, M. Souuflaoui, *Tetrahedron* **54** (1998) 8055-8064.

[35] R. Kumar, Y.C. Joshi, *Eur. J. Chem.* **4** (2007) 606-610.

[36] L.S. Gadekar, B.R. Arbad, M.K. Lande, *Chinese Chemical Letters* **21** (2010) 1053-1056.

[37] T. Yoshiyuki, Y. Kazuaki, Hokkaido Daigaku Koagakubu Kenkyu Hokoku, *Chemical Abstract* **93** (1980).

[38] C. Mukhopadhyay, A. Datta, *Heterocycles* **71** (2007) 1837-1842.

[39] M. Kodomari, Y. Tamaru, T. Aoyama, *Synthetic Communications* **34** (2004) 3029-3036.

[40] D.L. Boger, *Journal of Organic Chemistry* 43 (1978) 2296-2297.

[41] A. Teimouri, A. NajafiChermahini, H. Salavati, L. Ghorbanian, *Journal of Molecular Catalysis A: Chemical* **373** (2013) 38-45.

[42] A. Mobinikhaledi, N. Foroughifar, N. Basaki, *Turk J Chem* **33** (2009) 555-560.

[43] M. Zendehdel, A. Mobinikhaledi, H. Alikhani and N. Jafari, *Journal of the Chinese Chemical Society* **57** (2010) 683-689.

[44] P. Oxley, W.F. Short, *Journal of Chemical Society* (1947) 497-505.

[45] B. George, E.P. Papadopoulos, E. P. Journal of Organic Chemistry **42** (1977) 441-443.

[46] P. Gogoi, D. Konwar, *Tetrahedron Letters* **47** (2006) 79-82.

[47] S. Santra, A. Majee, A. Hajra, *Tetrahedron Lett* **53** (2012) 1974-1977.

[48] P. Ghosh, R. Subba. *Tetrahedron Letters* **56** (2015) 2691-2694.

[49] V. S. Padalkar, V. D. Gupta, K. R. Phatangare, V. S. Patil, P. G. Umape, N. Sekar, *Green Chemistry Letters and Reviews* **5** (2012) 139-145.

[50] H. Sharghi, O. Asemani, R. Khalifeh, *Synthetic Communicationsw* **38** (2008) 1128-1136.

[51] A. V. Narsaiah, A. R. Reddy, J. S. Yadav, *Synthetic Communications1* **41** (2011) 262-267.

[52] L. S. Gadekar, B. R. Arbad, M. K. Lande, *Chinese Chemical Letters* **21** (2010) 1053-1056.